Materials Science in Semiconductor Processing 147 (2022) 106672

Contents lists available at ScienceDirect

Materials Science in Semiconductor Processing

journal homepage: www.elsevier.com/locate/mssp

Investigation of temperature-dependent electrical parameters in a Schottky barrier diode with multi-walled carbon nanotube (MWCNT) interface

Hüseyin Ezgin [a,**], Ersin Demir [b], Selim Acar [c], Metin Özer [c,*]

[a] Department of Advanced Technologies, Gazi University, Ankara, 06500, Turkey
[b] Department of Analytical Chemistry, Afyonkarahisar Health Sciences University, Afyonkarahisar, 03030, Turkey
[c] Department of Physics, Gazi University, Ankara, 06500, Turkey

ARTICLE INFO

Keywords:
Schottky barrier diode
Electrical parameters
MWCNT
n-6H-SiC
Interface state density

ABSTRACT

We research the electrical parameters of the MWCNT/n-6H-SiC Schottky barrier diode (SBD) as a function of temperature. Voltage-dependent current and the capacitance measurements of the diode have been made between the temperatures of 300–480 K. The surface of the diode coated with CNT by drop drying method is examined by Scanning Electron Microscopy (SEM) and Raman Spectroscopy. It has been observed that MWCNTs coat on the semiconductor randomly and as entangled tubes, and the intensity in the D line is higher than in the G line. The ideality factor and barrier heights obtained from Thermionic Emission (TE) theory are in the range of 1.64–1.07 and 0.76–1.10 eV, respectively. The ideality factor and barrier heights of the produced diode are strongly related to temperature. By using Cheung-Cheung and Norde methods, series resistance, ideality factor, and barrier height parameters are calculated depending on temperature. It is effective in changing the series resistance of MWCNTs used as interface material. Capacitance-voltage (C–V) measurements of the MWCNT/n-6H-SiC Schottky barrier diode are made at different frequencies at 300 K and a frequency of 1 MHz depending on different temperature. The increase of the produced diode capacitance at low frequencies is associated with the interface states.

1. Introduction

Carbon nanotubes (CNTs) with diameters at the nanoscale are one-dimensional nanostructures made of carbon and in the form of a tube. They are defined as sheets of graphite rolled into cylindrical shapes. These graphite sheets are coiled and resemble a hexagon-like network structure. When the graphite sheets roll to form CNTs, not only are the carbon atoms arranged around the cylindrical shapes but also the quantum mechanical wavefunctions of the electrons are arranged harmoniously. Considering the number of carbon layers, they can have a single and multi-walled structure. Single-walled carbon nanotubes (SWCNTs) comprise of a single layer of graphene, usually hexagonally packed bundles, with diameters ranging from 0.4 to 2 nm. The diameter range of MWCNTs is 1–3 nm, and each graphite sheet consists of two or more cylindrical structures [1]. MWCNTs have a structure consisting of two or more SWCNTs with an intermediate layer that can act between carbon atoms in different walls by non-covalent van der Walls forces. Chemically, CNTs can be divided into two regions as edges and sidewalls. Depending on the molecular direction, the rolling graphite layer has three different shapes as an armchair, a zigzag, and a chiral [2]. Due to the nature of the bonds between carbon atoms, CNTs have ultra-lightweight, low density, high elasticity, high tensile strength, high thermal conductivity, and special electronic structures [3]. These interesting physical and chemical properties make CNTs valuable in fields as diverse as electronics, materials science, optics, nanotechnology, biotechnology, healthcare, and pharmaceuticals. Since carbon nanotubes have excellent electrical properties, they are used in high-performance diodes, field effect transistors (FETs), integrated circuits (IC), and sensors.

Despite being topologically simple, the metallic and semiconducting behavior of CNTs is interesting for electronic technologies. In this context, the interface states of the structures formed by CNTs with other materials can significantly affect the operation and performance of nanoscale electronic devices. Despite many studies on the interfacial behavior of CNTs and metals [3–8], the difficulty of contacting or forming contacts between CNTs and semiconductor (S) materials

* Corresponding author.
** Corresponding author.
E-mail addresses: huseyin.ezgin@gazi.edu.tr (H. Ezgin), metinoz@gazi.edu.tr (M. Özer).

https://doi.org/10.1016/j.mssp.2022.106672
Received 7 December 2021; Received in revised form 21 March 2022; Accepted 22 March 2022
Available online 23 April 2022

prevents detailed analysis of CNT/S device structures [9]. Besides, studies in which the electrical properties of CNT/S heterojunction Schottky barrier diodes (SBD) are analyzed depending on temperature are limited. Chen and Lue [10] investigated the variation of barrier height at the interface of aligned MWCNTs depending on temperature for field emission studies. They have reported that MWCTNs are not sensitive to the variation of field emission currents between the temperatures of 20–300 K. They have expressed that as the temperature decreases, the Fermi energy level increases as fewer electrons flow to the surface from metallic MWCNTs in the interface, therefore the barrier height in the interface decreases. Maruyama et al. [9] studied the energy band alignment in the interface among the CNT/n-6H-SiC heterojunction using photoelectron spectroscopy (PES). According to the PES results, it has been stated that the Schottky barrier has occurred at the interface of the heterojunction structure and the barrier height at room temperature is 1.38 eV. Uchino et al. [11] investigated on the electrical transport characterizations of the SWCNT/Si heterojunction diode structure in the temperature ranging of 50–300 K. They have determined that the diode show rectifying behavior, transitions from thermionic emission to tunneling currents are observed at the bias current at 150 K, and the barrier heights in the interface are obtained between 0.3 and 0.5 eV. Inaba et al. [12] researched the Schottky barrier heights for the Ti/CNT/SiC structure at different doping concentrations of SiC. They have reported that the barrier heights derived from the contact resistance ranged from 0.40 eV to 0.45 eV.

It is important that the Schottky barrier height (SBH) is low and high in different electronic device applications. For example, in transistor applications, a low-size Schottky barrier is preferred, which reduces contact resistance and has a good on/off ratio. In contrast, high-frequency applications such as sensors require a high barrier height with good rectifying properties. Studies on the electrical behavior of CNT/S Schottky device structures provide information about Schottky diode parameters and conductivity mechanisms at the interface of carbon nanotubes and other materials. From measurements of the electrical properties of SBDs at room temperature, no comprehensive information is provided about the nature, properties, and conduction function of the Schottky barrier occurring in the interface. In this context, temperature-dependent electrical measurements of SBDs allow us to have different perspectives on the conduction properties of these structures. In addition, the relationship between current and temperature in the device structures created reveals the existence of the Schottky barrier. The thermally activated current in a Schottky barrier increases with temperature. In this study, the electrical properties at the interface of the heterojunction structure formed by the pristine MWCNT and the n-type 6H-SiC semiconductor are investigated between the temperatures of 300–480 K.

2. Experimental procedure

In the production of Schottky barrier diode; n-type 6H-SiC semiconductor crystal from Cree Incorporation with 275 μm thickness, 2.6 × 10^{17} cm^{-3} donor concentration, and (0001) orientation was used as the substrate crystal. Before the ohmic contact was formed, the semiconductor crystal was chemically cleaned. Semiconductor crystal was put in isopropanol (C_3H_8O), acetone (C_3H_6O), and methanol (CH_3OH), respectively. Later, the crystal was kept in an ultrasonic bath for 5 min. After each stage, the crystal was washed with deionized water. For removing the natural oxide layer on the crystal, 1:10 HF + H2O solution was prepared and kept for 15 s. Next, the crystal was dried with pure nitrogen (99.99%) gas.

The chemically cleaned semiconductor was placed on the mask, whose interior was empty with its matte surface down. The mask was placed in the thermal evaporation system and the system was vacuumed up to a pressure of 10^{-6} mbar. The matte side of the semiconductor was coated with pure Au (99.995%) at a thickness of 170 nm. Then, the semiconductors were annealed under the same pressure and nitrogen environment at 400 °C for 3 min, allowing the Au film to precipitate into the SiC crystal. After this process, MWCNTs supplied in powder form (>90% carbon basis and O.D. 10–15 nm × I.D. 2–6 nm × L 0.1–10 μm size) from Sigma-Aldrich company were weighed as 2 mg and the suspension was prepared as a solution by placing them in 1 mL of dimethylformamide (DMF) (C_3H_7NO) solvent. The suspension solution formed was mixed in an ultrasonic bath at 50 °C for 2 h. The drop drying method, which is a chemical method, was used to coat CNTs on the polished surface of semiconductor [13–15].

20 μL of pristine MWCNT solution was coated on the front surface of the semiconductor. In order to clean the solution from the semiconductor surface, it was dried under −10 PSI vacuum at approximately 50 °C for 2 h. The semiconductor surface coated with CNT was placed on a mask with 1 mm diameter holes. The surface, which was placed in the thermal evaporation system, was covered with 180 nm thick pure Au (99.95%) under a pressure of 10^{-6} mbar and in a nitrogen environment. Since the MWCNTs coated on the SiC surface as an interface with an average thickness of 200 nm are of sufficient density, the diffusion of Au metal inside the MWCNTs can be neglected [9,12]. The representation of the produced Au/MWCNT/n-6H-SiC/Au SBD is in Fig. 1.

In the characterization of the diode structure produced, it was examined by Scanning Electron Microscopy (SEM) and Raman Spectroscopy. Current-voltage (I–V) and capacitance-voltage (C–V) properties were measured using Keithley 2400 Sourcemeter and Keysight E4990A Impedance Analyzer. As the relationship between the current and temperature of the produced diode shows the best diode characteristics in the voltage range from −3 V to +3 V in the 300–480 K temperature range with 20 K steps. Besides, C–V measurements were made at the same temperature and voltage ranges.

3. Results and discussion

SEM images of the MWCNT structure coated on SiC crystal are represented in Fig. 2. Since no alignment mechanism is used in the coated of CNTs to the crystal surface, the spaghetti-like tubes coat on the crystal surface in an entangled and random manner (Fig. 2a and b). The outer diameter of the CNTs varies between 17 and 22 nm (Fig. 2c), while the thickness taken from the cross-section of the coated layer is between 184 nm and 223 nm (Fig. 2d). The multi-walled CNT structure, which is initially in the form of spherical powder particles, softens with the effect of DMF solution and annealing temperature and then takes a cylindrical shape.

Raman spectra of the pristine MWCNT structure coated on SiC crystal surface are given in Fig. 3. 1350 and 1585 cm^{-1} peaks reveal the existence of the D line and G line, respectively. Higher-order lines of Raman peaks are mostly associated with primary-order D and G lines. Two more secondary lines are seen at 2696 and 2937 cm^{-1} peaks, which are not combinations of the D line and the G line. These observed peak values are in agreement with other studies reported on MWCNT in the literature [16–18]. The 1350 cm^{-1} signal indicating the D line in CNTs indicates the existence of amorphous or disordered carbon and expresses the disorder-induced vibrations of the C–C bonds [19]. The G line around the 1585 cm^{-1} peak is linked to the C–C carbon material frequency in the sp^2 orbital and corresponds to the E_{2g} optical mode of the structure. Since the structure of the material is highly crystalline, the density of the E_{2g} mode of graphite materials is strong and sharp [20]. As can be seen from Fig. 3, the intensity in the D line is higher than that of the G line ($I_D > I_G$). The fact that MWCNTs are exposed to further processing in DMF solution and their intensity in the D line is related to te the occurrence of defects on the surface. These defects occurring on the material surface cause some degree of irregularity in the CNT structure and an increase in the D line's intensity [21].

Main current-conduction mechanisms at the interface as a result of contacting a metal with a semiconductor can occur as thermionic emission (TE), tunneling across the barrier, space charge, generation, and recombination in the neutral region. For the voltage ranges

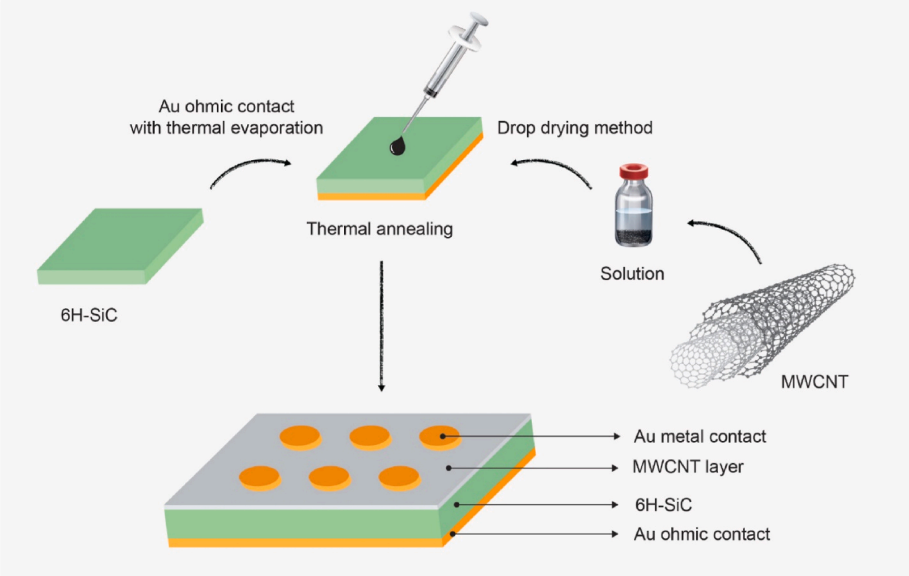

Fig. 1. The production stages and the cross-sectional view of the layers of the produced Au/MWCNT/n-6H-SiC/Au SBD.

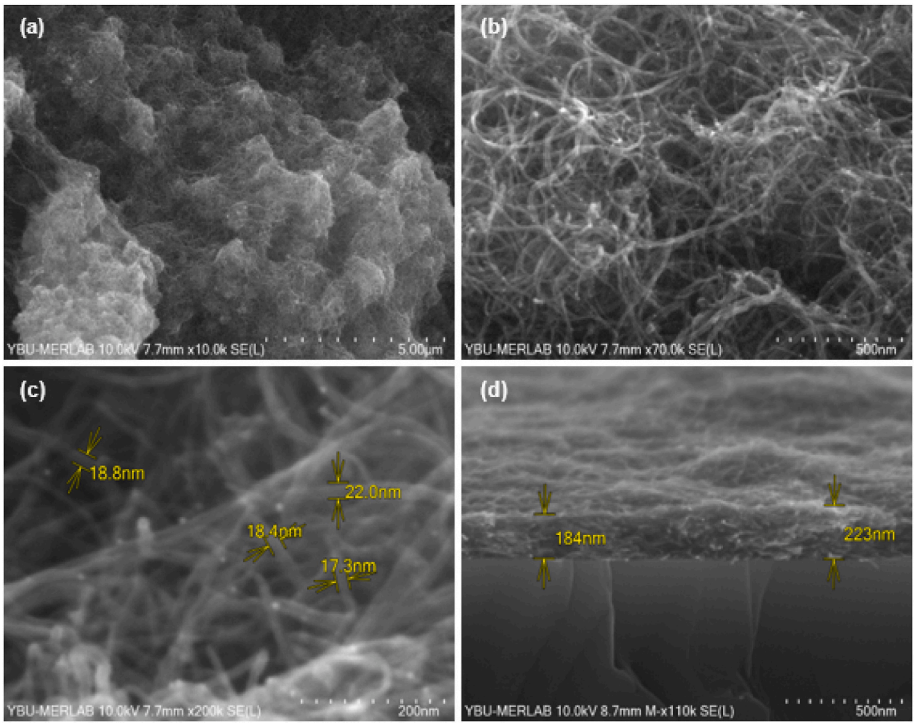

Fig. 2. (a) The SEM image of CNTs coated on crystal surface (b) the spaghetti-like and randomly distributed CNTs (c) the outer diameter of the CNTs varies between 17 and 22 nm (d) the cross-section of the coated layer.

measured for certain temperatures in Schottky diodes, not only one of the current conduction mechanisms may be dominant, but also the effect of more mechanisms can be seen. The high electron mobility of many semiconductors allows for the thermionic emission model to be considered as the basic current limitation, ignoring diffusion or drift currents in the depletion layer [22]. If the conduction mechanism in the Schottky barrier is thermionic emission, electrons flow from semiconductor to metal, and so the graph of current and voltage increases exponentially in case of forward bias. On the other hand, the device saturates since the metal-to-semiconductor barrier height does not change in the reverse bias state of the thermionic emission (TE). Considering the TE theory, the equation of the current in the forward bias Schottky barrier diode is given as

$$I = I_0 \exp\left(\frac{q(V - IR)}{nkT}\right)\left(1 - \exp\left(-\frac{q(V - IR)}{kT}\right)\right). \quad (1)$$

In this equation, the saturation current is I_0, the electron charge is q, the application voltage of the diode is V, IR the voltage drop due to the resistance of the diode. n, k, and T are the ideality factor, the Boltzman constant, and the absolute temperature, respectively. The expression for the saturation current is

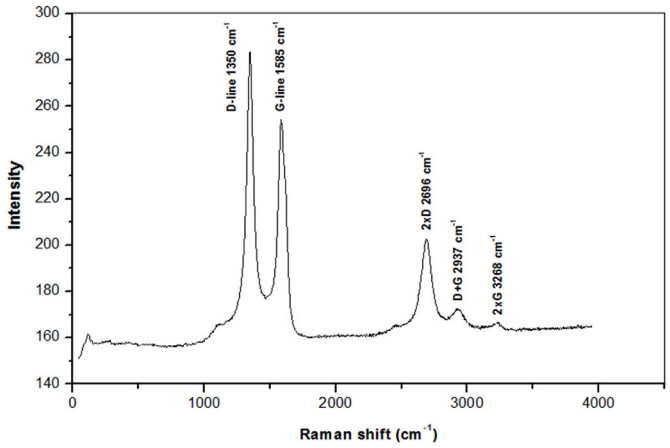

Fig. 3. Raman spectra of MWCNT coated on the n-6H-SiC substrate.

$$I_0 = AA^* \exp\left(\frac{-q\Phi_{b0}}{kT}\right). \quad (2)$$

The value of I_0 is obtained from the point that intersects the vertical axis in the linear region of the LnI-V graph. The diode area is the term A in the equation, Richardson's constant is A^*, and the barrier height at zero bias is Φ_{b0}. Richardson's constant value for n-6H-SiC semiconductor is taken as 146 $Acm^{-2}K^{-2}$ [23,24]. The barrier height expression from Eq. (2) is written as

$$\Phi_{b0} = \frac{kT}{q} \ln\left(\frac{AA^*T^2}{I_0}\right). \quad (3)$$

The ideality factor value is found from the forward bias curve within the linear part of the LnI-V graph and the expression of n is

$$n = \frac{q}{kT} Ln\left(\frac{d(V - IR)}{d(lnI)}\right). \quad (4)$$

If the graph is nonlinear, the value of n is larger than 1 and the TE theory alone as the current conduction mechanism of the diode is not valid. The recombination currents inside the depletion area can cause this situation.

The semi-log experimental I–V graph of the produced Au/MWCNT/n-6H-SiC/Au Schottky barrier diode (SBD) between 300 and 480 K temperature values are shown in Fig. 4. It is observed that the diode produced by using MWCNT between Au and n-6H-SiC forms a Schottky barrier. Considering the TE model, n value is derived from the slope of the LnI-V graph, and Φ_{b0} at zero bias is calculated from the intersection of the graph. It is determined that the n values of the produced diode at 300 and 480 K temperatures are 1.64 and 1.07, and Φ_{b0} values are 0.76 and 1.10 eV, respectively. The graph showing the variation of n and Φ_{b0} parameters with temperature is presented in Fig. 5. Güzel et al. [25] calculated n and Φ_b values of the Au/n-6H-SiC SBD between the temperatures of 80–400 K. They reported that n is in the range of 6.4 to 1.8 and Φ_b is in the range of 0.22–0.78 eV. The n values range from 2.1 to 1.8 and the Φ_b values range from 0.68 to 0.78 eV for temperatures of 300–400 K. Sefaoglu et al. [26] determined that n is in the range of 1.70 to 1.16, and Φ_b is in the range of 0.65–1.27 eV for the Ni/n-6H-SiC SBD between the temperatures of 100–500 K. The n values vary between 1.27 and 1.16, and Φ_b values vary between 1.05 and 1.27 eV for temperatures of 300–500 K. Kaya et al. [27] found that n is in the range of 3.41 to 1.64, and Φ_b is in the range of 0.39–0.90 eV for the Ni/n-6H-SiC SBD between the temperatures of 100–500 K. The n values are in the ranging of 1.91–1.64 and the Φ_b values are in the ranging of 0.76–0.90 eV for temperatures of 300–400 K. When the results of these diodes are compared with the results obtained from our study, it is seen that the ideality factor obtained from our study is lower than the Au/n-6H–SiC diodes, and it is slightly higher for the Ni/n-6H-SiC diode.

As can be seen in Fig. 5, Φ_{b0} increases while n decreases with increasing temperature. That is, while the n ideality factor exhibits an inversely proportional relationship with the temperature, the Φ_{b0} barrier height reveals a directly proportional relationship with the temperature. This result proves that n and Φ_{b0} parameters have a strong correlation with temperature. Since current conduction across the interface of the diode is temperature-associated, current generation occurs by carriers that cross the Schottky barrier, and since the temperature increases, more electrons have enough energy to cross the Schottky barrier. The higher ideality factor for MWCNT/n-6H-SiC diode can be clarified by the presence of surface defects of the MWCNT structure at the interface, the inhomogeneous Schottky barrier, and the dependence of the barrier height on the supply voltage [28]. On the other hand, the effect of recombination and tunneling currents can be seen in the larger values of the ideality factor [28,29].

In the LnI-V graph, the low voltage regions of the forward bias current generally show a linear behavior. When the voltage is increased, deviations occur in the linear region of the graph. These deviations are due to the interface material used in the diode and the resistance caused by the interface states. In this context, one of the essential parameters to recognize the electrical features of Schottky diodes is the series resistance (R_S). The Cheung-Cheung method is one of the methods for determining the series resistance. Besides R_S value, n and Φ_{b0} parame-

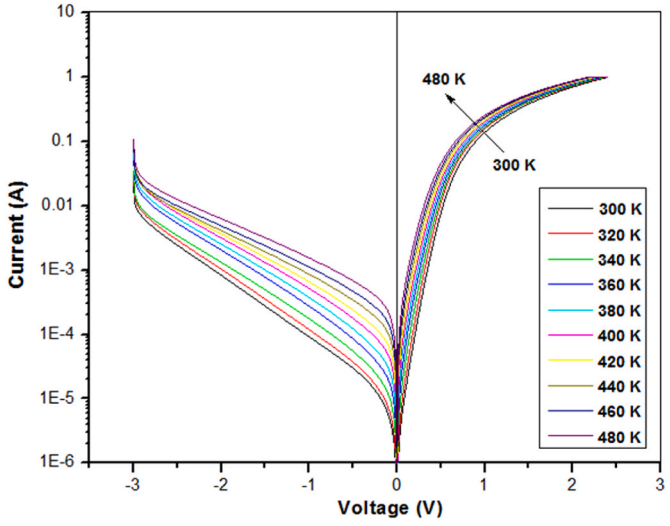

Fig. 4. The semi-logarithmic I–V graph for Au/MWCNT/n-6H-SiC/Au SBD in both forward and reverse bias current between the temperatures of 300–480 K.

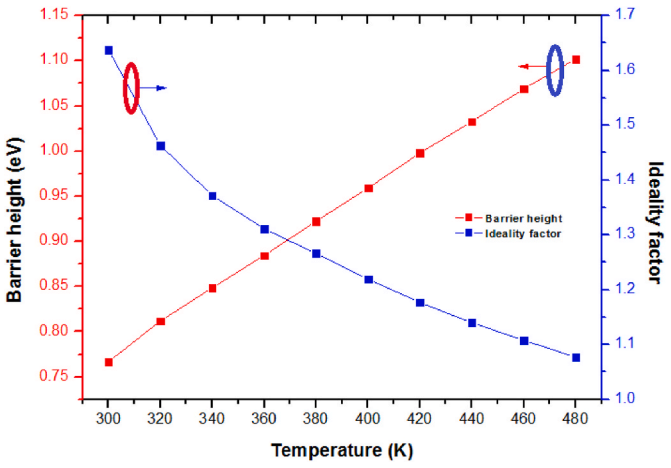

Fig. 5. The graph of n and Φ_{b0} for Au/MWCNT/n-6H-SiC/Au SBD depending on the temperature at zero bias between the temperatures of 300–480 K.

ters are also determined in this method. R_s is described by [30].

$$\frac{dV}{d(\ln I)} = \frac{nkT}{q} + IR_S, \tag{5}$$

$$H(I) = IR_S + n\Phi_{b0}. \tag{6}$$

$\frac{dV}{d(\ln I)}$ - I graph is presented in Fig. 6. While the slope of this graph gives the R_S value, the n value is obtained from the intersection of the graph with the y-axis.

While the R_S value is obtained from the slope of H(I) - I graph presented in Fig. 7, $n\Phi_{b0}$ value is found from the intersection of the graph. The value of Φ_{b0} is determined from this intersection point of the graph. Table 1 includes the electrical properties derived from the Cheung-Cheung method for MWCNT/n-6H-SiC SBD.

Another approach developed for the calculation of R_S is the Norde method [31]. The method is also a convenient method for calculating the barrier height of the diode. The disadvantage of the method is that it's hard to determine the minimum point on the graph. The Norde function expression is

$$F(V) = \frac{V}{\gamma} - \frac{1}{\beta}\ln\left(\frac{I(V)}{AA^*T^2}\right). \tag{7}$$

The value of γ in the function is an arbitrary integer larger than the ideality factor, and the value of β is q/kT. As seen in Fig. 8, there are minimum points for each temperature value in F(V) - V graph. The barrier height is obtained through the following equation,

$$\Phi_b = F_{min} + \frac{V_{min}}{\gamma} - \frac{1}{\beta}. \tag{8}$$

In this equation, V_{min} is the value corresponding to F_{min} on F(V) - V graph. The equation giving R_S,

$$R_S = \frac{\beta(\gamma - n)}{I_{min}}. \tag{9}$$

Experimental results with the Norde method are shown in Table 2. According to Table 1 and Table 2, when the series resistance values obtained from Cheung-Cheung and Norde methods are compared with each other, there is some difference at temperatures close to room temperature. The series resistance values determined from the Norde method, it is higher between the temperatures of 300–420 K compared to the Cheung-Cheung method. The R_s values of both methods have closer values to each other in the temperature range of 420–480 K. The difference in results is due to the computational difference between the

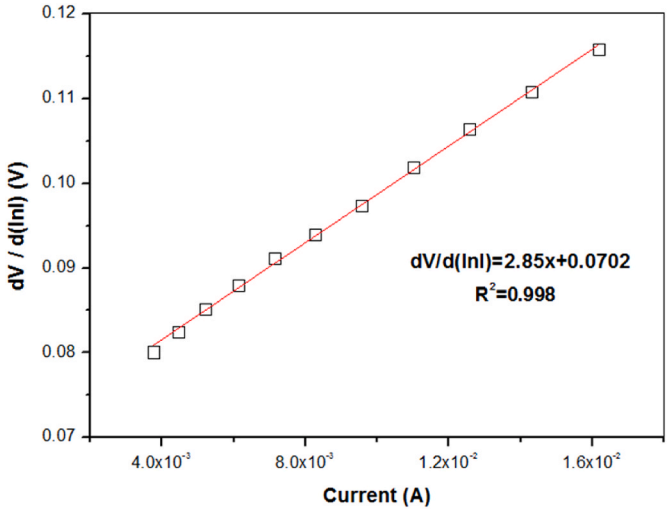

Fig. 6. dV/d(lnI) vs current graph of Au/MWCNT/n-6H-SiC/Au SBD at room temperature.

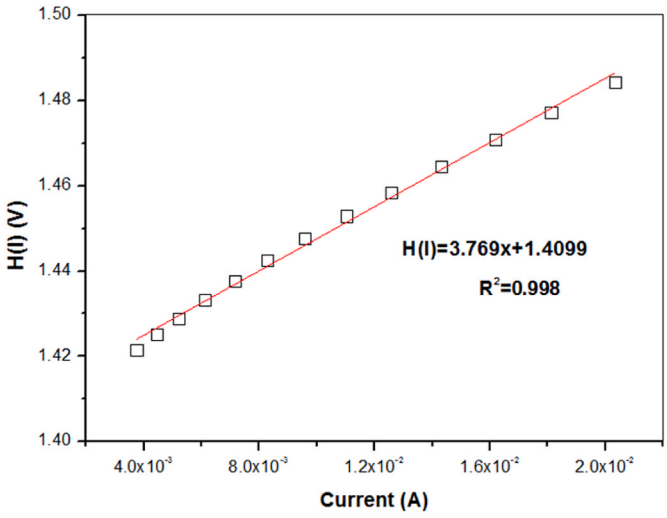

Fig. 7. H(I) vs current graph of Au/MWCNT/n-6H-SiC/Au SBD at room temperature.

Table 1
R_S, n, and Φ_{b0} values calculated by Cheung-Cheung method for Au/MWCNT/n-6H-SiC/Au SBD.

T (K)	R_S (Ω) dV/dln(I)–I	n dV/dln(I)–I	R_S (Ω) H(I)–I	Φ_{b0} (eV) H(I)–I
300	2.85	2.71	3.77	0.51
320	2.59	2.56	2.97	0.56
340	2.46	2.55	2.83	0.59
360	2.34	2.53	2.57	0.61
380	2.22	2.46	2.34	0.65
400	2.07	2.44	2.17	0.67
420	1.93	2.42	2.00	0.70
440	1.84	2.39	1.85	0.73
460	1.81	2.30	1.76	0.78
480	1.73	2.27	1.69	0.81

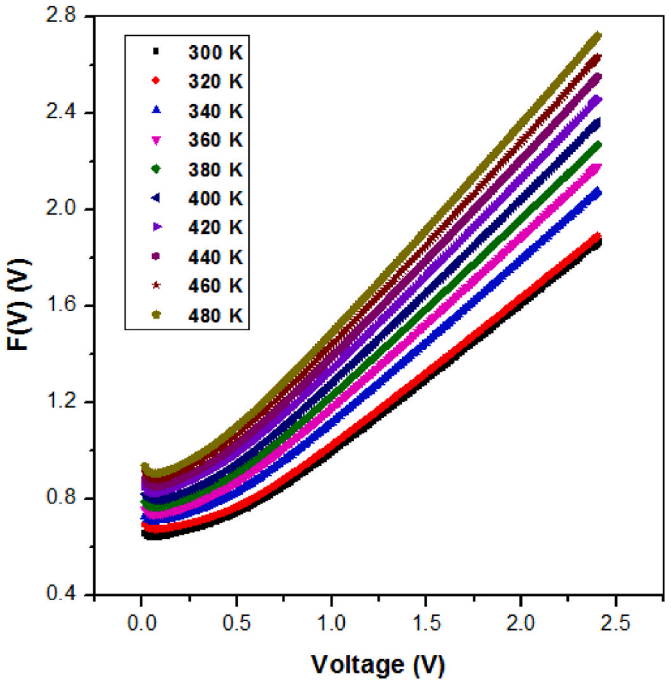

Fig. 8. F(V) vs voltage plots of Au/MWCNT/n-6H-SiC/Au SBD between the temperatures of 300–480 K.

Table 2
R_S, n, and Φ_{b0} values calculated by the Norde method for Au/MWCNT/n-6H-SiC/Au SBD.

T (K)	R_S (Ω) F(V)–V	Φ_{b0} (eV) F(V)–V
300	75.4	0.66
320	27.8	0.70
340	19.9	0.73
360	11.7	0.76
380	7.74	0.79
400	5.33	0.82
420	3.57	0.85
440	2.55	0.87
460	1.85	0.90
480	1.27	0.93

two methods.

According to the results, it is seen that the value of R_S decreases with increasing temperature. The higher R_S values around room temperature in the MWCNT/n-6H-SiC diode may be associated with a decrease in the free charge carrier concentration in the interface. Decreasing the charge carrier concentration can increase the value of R_S [32]. Because charge carriers with higher mobility in the interfacial layer can conduct more freely towards metal. The temperature-dependent R_S values of the MWCNT/n-6H-SiC diode are lower than the previously reported Au/n-SiC structures [25,27]. The MWCNT interface is effective in reducing the series resistance.

One of the alternative methods used to derive the barrier height is the Richardson plot [33]. The Richardson plot is presented in Fig. 9 for our produced SBD. The equation that gives this plot is

$$\ln\left(\frac{I_0}{T^2}\right) = \ln(AA^*) - \frac{q\Phi_{b0}}{kT}. \quad (10)$$

$\ln(I_0/T^2)$ vs 1000/T graph obtained from the equation is foreseen to be linear. While the slope of the graph gives the barrier height at 300 K, the obtained value is likewise the activation energy of the diode. Richardson's constant (A^*) is found from the intersection of the graph with the slope line. A^* and Φ_{b0} calculated from the MWCNT/n-6H–SiC diode are 5.84 × 10^{-6} $Acm^{-2}K^{-2}$ and 0.21 eV, respectively. The difference of A^* calculated from the temperature-dependent I–V properties and the theoretical results can be linked with the spatial inhomogeneity of the barrier height at the diode interface and regional potential fluctuations. In the potential distribution of the diode, the current prefers to flow through the lower barrier height [24,34]. During the conduction of current, a situation may arise where the effective mass may be different as the diode passes through different potential barrier heights. Therefore, A^* may differ from the theoretically obtained data due to the deviation in the calculated effective mass [35]. A^* value found for MWCNT/n-6H-SiC produced for this study has similar values and shows compatibility with different studies [36,37].

The graph of n versus the experimental Φ_{bo} of MWCNT/n-6H-SiC diode is shown in Fig. 10. A linear relationship is derived between the effective barrier height and the ideality factor, which indicates that the barrier is not homogeneous. Homogeneous barrier heights are determined from the point where the barrier height intersects the axis for a value of n = 1. The effective barrier height (Φ_e) of the produced MWCNT/n-6H-SiC SBD between temperatures of 300–480 K is derived as 1.11 eV. The results found show that the current conduction mechanism deviates from the TE model. The reason for this deviation can be expressed by the inhomogeneity of the barrier heights of the diode.

The capacitance-voltage properties of MWCNT/n-6H-SiC SBD in the forward and reverse bias current at 300 K are presented in Fig. 11. The measured diode capacitance at frequencies of 5, 10, 50, 100, 500, and 1000 kHz decreases as the frequency values increase. The capacitance increase at low-frequency values can be associated with the interface states. The interface states at low frequencies follow the alternating current signal. Thus, the depletion capacitance and the interface state capacitance appear directly in parallel, which further increases the total capacitance [38]. Since the frequency increases, the interface states cannot act relative to the alternating current and the interface states take fixed values. The charges of the interface state that don't make contributions to the diode capacitance cause the capacitance to take low values [39].

The C–V properties of the capacitance, which can be computed from the reverse bias current, measured at 1 MHz frequency in the 300–480 K temperature range are shown in Fig. 12. The depletion layer capacitance in Schottky diodes is defined as follows [28].

$$\frac{1}{C^2} = \frac{2(V_0 + V_R)}{q\varepsilon_s A^2 N_d}. \quad (11)$$

A term in this equation is the contact area. The permittivity of the n-6H-SiC semiconductor crystal is ε_s and $\varepsilon_s = 9.6\ \varepsilon_0$ (The permittivity of free space is ε_0). The donor or free carrier concentration is N_d. The reverse voltage is V_R and the cutting voltage is V_0. Diffusion potential (V_d) is calculated by using V_0 determined by extending C^{-2}-V curves to the potential axis. In the absence of interface states, there is a $V_0 = V_d - kT/q$ relationship between cutting voltage V_0 and diffusion voltage V_d. The values of V_d and N_d are found as 1.13 V and 2.13 × 10^{+15} cm^{-3},

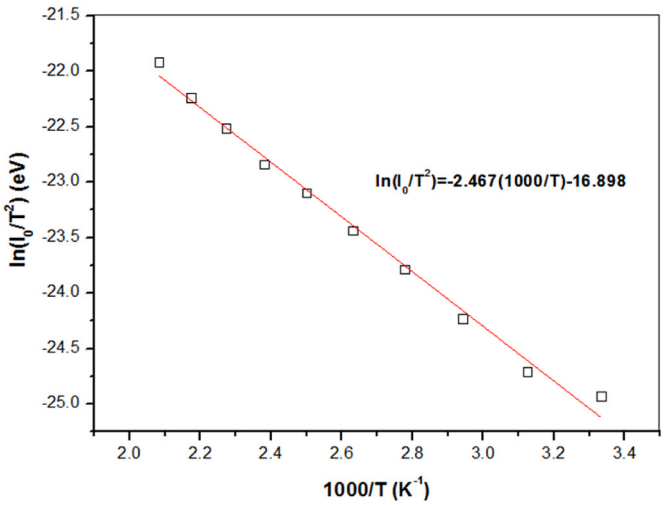

Fig. 9. The Richardson plot for Au/MWCNT/n-6H-SiC/Au SBD.

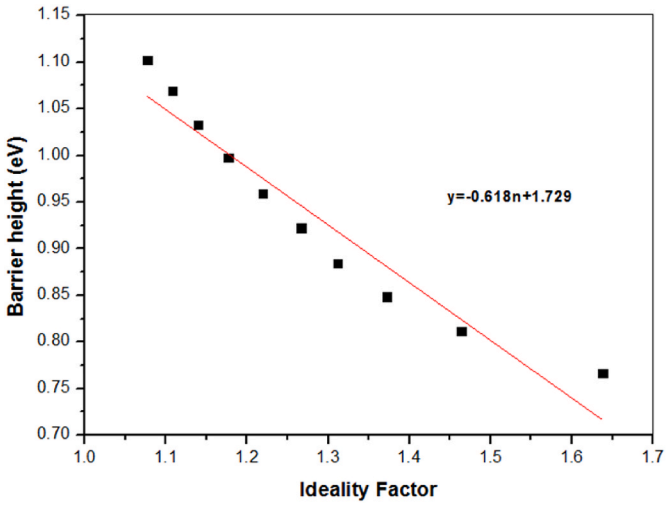

Fig. 10. The barrier height vs the ideality factor at zero bias for Au/MWCNT/n-6H-SiC/Au SBD between the temperatures of 300–480 K.

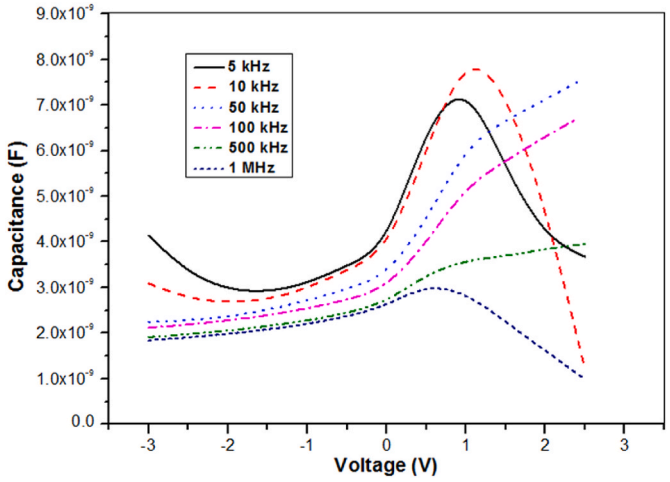

Fig. 11. C–V features of Au/MWCNT/n-6H-SiC/Au SBD measured for different frequencies at 300 K.

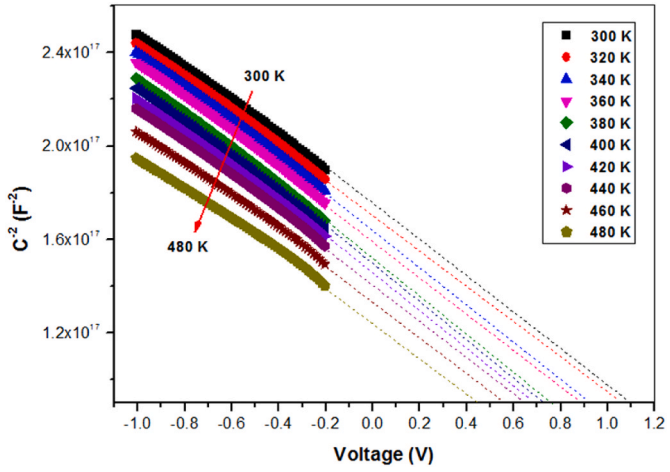

Fig. 12. C^{-2}-V plots at reverse bias for Au/MWCNT/n-6H-SiC/Au SBD between the temperatures of 300–480 K.

respectively, in the zero bias condition at 300 K.

The equation from which the barrier height is obtained

$$\Phi_{b0}(C-V) = V_0 + V_n. \tag{12}$$

In this equation, V_n is the potential difference between the Fermi level and the minimum of the conduction band, which can be obtained by knowing the N_d donor concentration. V_n is given as

$$V_n = \frac{kT}{q}\ln\left(\frac{N_c}{N_d}\right), \tag{13}$$

in which the active state density in the conduction band is N_c and its value at 300 K for the n-6H-SiC semiconductor is $8.98 \times 10^{+19}$ cm^{-3} [40,41]. The experimental parameters found using the C–V data of the MWCNT/n-6H-SiC SBD are presented in Table 3.

According to Table 3, Φ_{b0} values measured from I–V increase depending on temperature, while Φ_{b0} values obtained from C–V measurement decrease with temperature. The values measured from I–V are more correlated with currents passing through lower barrier height. Therefore, the current measured is the current flowing through obstacles with low barrier height. In other words, depending on the temperature increase, more electrons with sufficient thermal energy will make the diode more easily overcome higher barrier heights. Because electrons with higher energy are more likely to cross the barrier. I–V measurements are affected by potential fluctuations at the interface. Because the current flowing through the interface in I–V measurement is exponentially dependent on the potential distribution of the barrier height in the interface [39]. On the other hand, capacitance measurements are insensitive to potential fluctuations at a smaller length scale in the space charge region. The barrier heights measured from C–V are related to the charge distributions in the depletion region of the diode. Φ_{b0} is related to the capacitance measured over the entire diode area. The reason for the difference between the values of Φ_{b0} in both I–V and C–V estimations may take place as a result of the inhomogeneity of the interface layer used in the device production, the inhomogeneity in the interfacial layer's thickness, and the uneven distribution of the carrier charges due to the defects at the interface. The Φ_{b0} values determined from C–V for MWCNT/n-6H–SiC SBD decrease as the temperature increases in the range of 300–480 K. The reason for behavior obtained from C–V can be associated with the decrease in the forbidden energy band gap of the SiC with increasing temperature and the number of carrier electrons in the space charge region [42,43].

Apart from the current conduction mechanisms, the interfacial layer's thickness and the interface state density affect the electrical parameters of the semiconductors in Schottky diodes. The interface state density has an important role in obtaining both the ideality factor and the barrier height. When the interfacial layer of the diode becomes thicker, the probability of conducting current decreases. Therefore, the Φ_e varies relying on the voltage applied to the diode. The effective barrier height is expressed by Ref. [44]:

$$\Phi_e = \Phi_{bo} + \beta V, \tag{14}$$

in which β is the voltage coefficient of the barrier height. This parameter is that consists of the impact of each interface state in equilibrium with the semiconductor. If $\beta = 1 - (1/n(V))$ is written in Eq. (14), Φ_e is given as

Table 3
Electrical parameters calculated from reverse-biased C^{-2}-V plot for Au/MWCNT/n-6H-SiC/Au SBD between the temperatures of 300–480 K.

T (K)	V_0 (V)	V_d (eV)	V_n (eV)	N_d (cm^{-3})	W_d (eV)	Φ_{b0} (eV) C–V	Φ_{b0} (eV) I–V
300	1.10	1.13	0.275	$2.13 \times 10^{+15}$	7.48×10^{-5}	1.38	0.76
320	1.07	1.10	0.296	$2.13 \times 10^{+15}$	7.39×10^{-5}	1.37	0.81
340	0.92	0.95	0.321	$1.86 \times 10^{+15}$	7.35×10^{-5}	1.24	0.85
360	0.88	0.91	0.343	$1.86 \times 10^{+15}$	7.20×10^{-5}	1.22	0.88
380	0.75	0.78	0.365	$1.86 \times 10^{+15}$	6.68×10^{-5}	1.12	0.92
400	0.72	0.74	0.386	$1.86 \times 10^{+15}$	6.55×10^{-5}	1.11	0.96
420	0.68	0.72	0.408	$1.86 \times 10^{+15}$	6.39×10^{-5}	1.09	1.00
440	0.63	0.67	0.431	$1.86 \times 10^{+15}$	6.16×10^{-5}	1.06	1.03
460	0.54	0.58	0.453	$1.86 \times 10^{+15}$	5.74×10^{-5}	0.99	1.07
480	0.42	0.46	0.470	$2.13 \times 10^{+15}$	4.89×10^{-5}	0.89	1.10

$$\Phi_e = \Phi_{bo} + \left(1 - \frac{1}{n(V)}\right)V. \quad (15)$$

The ideality factor expression n(V), which changes depending on the applied voltage, is defined by Card and Rhoderick as follows [27].

$$n(V) = 1 + \frac{\delta}{\varepsilon_i}\left(\frac{\varepsilon_s}{W_d} + qN_{ss}(V)\right). \quad (16)$$

By subtracting the N_{ss} term from Eq. (16), the following equation is obtained

$$N_{ss}(V) = \frac{1}{q}\left[\frac{\varepsilon_i}{\delta}(n(V) - 1) - \frac{\varepsilon_s}{W_d}\right], \quad (17)$$

where the interface state density is N_{ss}, the dielectric constants of the interface and the semiconductor are ε_i and ε_s, the thickness of an interfacial layer is δ, and the width of the consumption layer is W_d. The width of the consumption layer for each measured temperature is

$$W_d = \sqrt{\frac{2\varepsilon_s(V_0 + V_R)}{qN_d}}. \quad (18)$$

E_{ss} is the energy of the interface states for the n-type semiconductor and E_c is the conduction band boundary energy of the semiconductor surface. The difference between the surface of the semiconductor and the boundary of the conduction band is given below

$$E_c - E_{ss} = q(\Phi_e - V). \quad (19)$$

With the help of Eq. (16) together with Eq. (15) and Eq. (19), the interfacial state concentration distribution of the produced diode is calculated. In Fig. 13, the graph of versus N_{ss} is presented in the 300–480 K temperature range. The interface state density is between $1.57 \times 10^{+13}$ and $7.18 \times 10^{+13}$ $eV^{-1}cm^{-2}$ at 300 K and between $9.26 \times 10^{+12}$ and $6.27 \times 10^{+13}$ $eV^{-1}cm^{-2}$ at 480 K. As expected, these values indicate that N_{ss} decreases as the temperature increases. The fact that N_{ss} decreases with increasing temperature means that the ideality factor decreases as a function of temperature because of the inhomogeneity in barrier height at the interface of metal and semiconductor. In Schottky diodes, the material used in the interface layer, the series resistance effect, and the interface states are important in terms of barrier height. The lowering of N_{ss} with the effect of temperature can be explained by the reordering and restructuring of the interface with the effect of temperature [45].

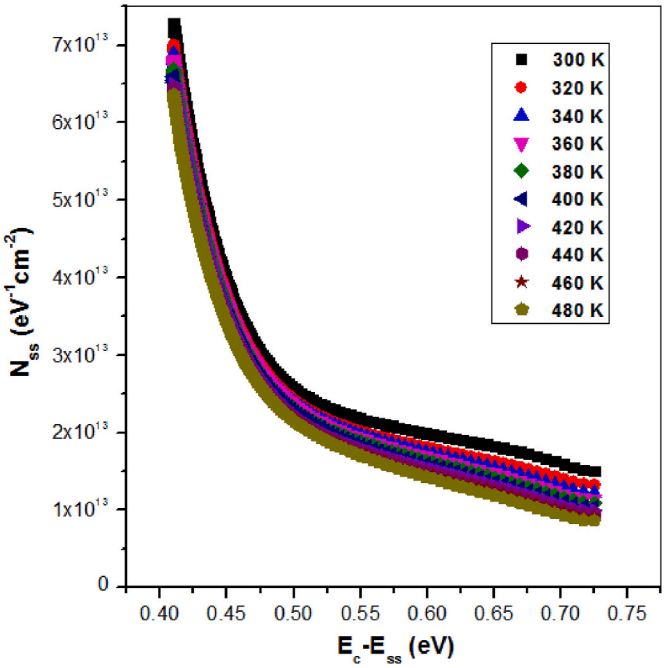

Fig. 13. N_{ss} vs E_c-E_{ss} plots of Au/MWCNT/n-6H-SiC/Au SBD between the temperatures of 300–480 K.

Forming contacts between SiC and CNTs with high electrical conductivity and examining the interface properties of this contact structure may have important effects on the operation and performance of electronic devices. Although there have been few studies showing that charge transfer is possible between SiC and CNTs, the development of different production methods other than the methods used allows a better understanding of the electronic properties of MWCNT/SiC devices. While the contacts formed with SiC and metals show rectifying behavior, the interface layer between SiC and metal affects the electrical properties of the diode. The materials used in the interface layer play a role in controlling the barrier height and changing the series resistance. MWCNTs are an alternative material to provide these electrical properties. The MWCNT/n-6H-SiC structure shows a distinctly rectifying behavior. It is observed that the current from MWCNTs to SiC increases linearly with the applied voltage, while a small amount of current goes from SiC to MWCNTs in reverse bias. This indicates that the MWCNT/n-6H-SiC structure forms the Schottky barrier. Considering the conductivity properties of both SiC and MWCNTs, the transfer of electrons from SiC to MWCNTs and from MWCNTs to metal is expected to be faster at the interface. However, barrier heights are slightly higher than other studies with Au/n-6H-SiC contact reported in the literature [25,27]. The large barrier height may be due to the atomic bond formation between SiC and MWCNTs. The carbon atoms in MWCNT form covalent bonds with the Si and C atoms in the SiC semiconductor. These bonds allow electron transfer between MWCNTs and SiC to occur. Also, it is seen that MWCNTs have an effect on the decrease in the series resistance values calculated from the Norde and Cheung-Cheung methods (Table 1 and Table 2). The series resistance values were significantly decreased compared to the previously reported Au/n-SiC structures [25,27]. On the other hand, there are a few studies in which CNT/SiC structure was formed and Schottky barrier formation was observed. Maruyama et al. [9] measured the Schottky barrier formed at the CNT/n-6H-SiC interface using PES and reported the potential barrier height at room temperature as 1.38 eV. Again, Inaba et al. [12] produced the Ti/CNT/SiC structure using the FIB (Focused Ion Beam) technique and determined that the barrier heights from the contact resistance were 0.40–0.45 eV by limiting the conduction area. In both studies, a dual barrier height formation is detected at the CNT/SiC interface and this situation is discussed. In our study, unlike these studies, a single barrier height formation was observed and the potential barrier height was determined as 0.76 eV at room temperature. In our opinion, the difference between potential barriers may depend on the type of CNTs used, the method of forming the CNTs at the interface, and the atomic bond structure between the CNTs and SiC. However, it is observed that the barrier heights are lower than many metal/n-6H-SiC structures [46,47]. This allows CNT/SiC structures produced by different methods to be used in different electronic device applications.

4. Conclusion

In summary, the electrical features of the produced MWCNT/n-6H-SiC Schottky barrier diode in the 300–480 K temperature range are investigated with I–V and C–V measurements as a function of temperature. In the surface characterization of MWCNTs coated on n-6H–SiC semiconductor by drop drying method, it is observed that MWCNTs are coated as random and entangled tubes on the semiconductor and the density in the D line is higher than that in the G line. It is determined that the ideality factor of the produced diode and the barrier heights in the zero bias state are strongly related to the temperature. Moreover, it has been determined that the series resistance values estimated by the

Cheung-Cheung and Norde methods are dependent on the temperature and R_S values are lower than the diodes without CNT. The decrease in R_S value with the increase in temperature is associated with the decrease in the free charge carrier concentration at the interface. The Richardson's constant of the Schottky diode and the average barrier height are calculated using the Richardson plot, which is an alternative approach used to obtain the barrier height. The results obtained show that the current conduction mechanism deviates from the TE model and the reason for this deviation can be ascribed to the inhomogeneous barrier heights of the diode. The capacitance-voltage estimations of the MWCNT/n-6H-SiC SBD in the forward and reverse bias current are measured depending on the frequency, and it is observed that the capacitance of the diode increased with decreasing frequency. There is a slight difference between the barrier height values in I–V and C–V measurements. This difference may come about as a result of the inhomogeneity of the interface layer and the uneven distribution of the carrier charges due to the defects at the interface. The temperature-dependent energy distribution of the interface state density (N_{ss}) is specified according to the forward bias state of the I–V measurements, taking into account the ideality factor and the bias dependence of the effective barrier height. N_{ss} tends to decrease with increasing temperature.

CRediT authorship contribution statement

Hüseyin Ezgin: Writing – review & editing, Writing – original draft, Visualization, Methodology, Investigation, Formal analysis, Conceptualization. **Ersin Demir:** Writing – review & editing, Methodology. **Selim Acar:** Writing – review & editing, Methodology. **Metin Özer:** Writing – review & editing, Writing – original draft, Supervision, Methodology, Investigation, Formal analysis, Conceptualization.

Declaration of competing interest

The authors declare that they have no known competing financial interests or personal relationships that could have appeared to influence the work reported in this paper.

Acknowledgment

We would like to thank Photonics Application and Research Center in Gazi University for contributing to the enlargement of the contacts on the diode and to Professor Doctor Recai İnam, who assisted in the realization of chemical processes in this research.

References

[1] N. Anzar, R. Hasan, M. Tyagi, N. Yadav, J. Narang, Carbon nanotube - a review on synthesis, properties and plethora of applications in the field of biomedical science, Sens. Int. 1 (2020) 100003.
[2] H. He, L.A. Pham-Huy, P. Dramou, D. Xiao, P. Zuo, C. Pham-Huy, Carbon nanotubes: applications in pharmacy and medicine, BioMed Res. Int. (2013) 578290.
[3] J. Kim, J.- O Lee, H. Oh, K.-H. Yoo, J.-J. Kim, Temperature dependence of the current-voltage characteristics of a carbon-nanotube heterojunction, Phys. Rev. B 64 (2001) 161404 (R).
[4] S.H. Jung, S.H. Jeong, S.U. Kim, S.K. Hwang, P.S. Lee, K.H. Lee, J.H. Ko, E. Bae, D. Kang, W. Park, H. Oh, J.J. Kim, H. Kim, C.G. Park, Vertically aligned carbon-nanotube arrays showing Schottky behavior at room temperature, Small 1 (2005) 553–559.
[5] W. Zhu, E. Kaxiras, The nature of contact between Pd leads and semiconducting carbon nanotubes, Appl. Phys. Lett. 89 (2006) 243107.
[6] F. Banhart, Interactions between metals and carbon nanotubes: at the interface between old and new materials, Nanoscale 1 (2009) 201–213.
[7] M.S. Wang, D. Golberg, Y. Bando, Interface dynamic behavior between a carbon nanotube and metal electrode, Adv. Mater. 22 (2010) 93.
[8] J. Svensson, E.E.B. Campbell, Schottky barriers in carbon nanotube-metal contacts, J. Appl. Phys. 110 (2011) 111101.
[9] T. Maruyama, S. Sakakibara, S. Naritsuka, W. Norimatsu, M. Kusunoki, H. Yamane, N. Kosugi, Band alignment of a carbon nanotube/n-type 6H-SiC heterojunction formed by surface decomposition of SiC using photoelectron spectroscopy, Appl. Phys. Lett. 101 (2012), 092106.
[10] S.-Y. Chen, J.-T. Lue, Temperature dependence of interface barrier height change as implicated by field emission studies of aligned-multiwall carbon nanotubes, Phys. Lett. 309 (2003) 114–120.
[11] T. Uchino, F. Shimpo, T. Kawashima, G.N. Ayre, D.C. Smith, C.H. de Groot, P. Ashburn, Electrical transport properties of isolated carbon nanotube/Si heterojunction Schottky diodes, Appl. Phys. Lett. 103 (2013) 193111.
[12] M. Inaba, K. Suzuki, M. Shibuya, C.-Y. Lee, Y. Masuda, N. Tomatsu, W. Norimatsu, A. Hiraiwa, M. Kusunoki, H. Kawarada, Very low Schottky barrier height at carbon nanotube and silicon carbide interface, Appl. Phys. Lett. 106 (2015) 123501.
[13] N. Hu, Y. Wang, J. Chai, R. Gao, Z. Yang, E.S.-W. Kong, Y. Zhang, Gas sensor based on p-phenylenediamine reduced graphene oxide, Sensor. Actuator. B Chem. 163 (2012) 107–114.
[14] G. Solleti, P. Jeevankumar, N. Jayarambabu, A. Sineetha, K.K. Sadasivinu, Satish Bykkam, K.V. Rao, Investigation of various $Mg_{(x)}Fe_{(1-x)2}O_4$ ($x = 0.1$, 0.5 and 0.9) nanostructures as a resistive and flexible LPG sensor, Mater. Sci. Eng., B 225 (2020) 114515.
[15] T. Li, M. Ichimura, Fabrication of transparent $Mg(OH)_2$ thin films by drop-dry deposition, Materials 14 (2021) 724.
[16] M. Sveningsson, R.-E. Morjan, O.A. Nerushev, Y. Sato, J. Bäckström, E.E. B. Campbell, F. Rohmund, Raman spectroscopy and field-emission properties of CVD-grown carbon-nanotube films, Appl. Phys. A 73 (2001) 409–418.
[17] M. Bansal, R. Srivastava, C. Lal, M.N. Kamalasanan, L.S. Tanwar, Change in conformation of polymerPFO on addition of multiwall carbon nanotubes, Nanoscale 2 (2010) 1171–1177.
[18] H. Javed, M. Islam, N. Mahmood, A. Achour, A. Hameed, Nasrullah Khatri, Catalytic growth of multi-walled carbon nanotubes using $NiFe_2O_4$ nanoparticles and incorporation into epoxy matrix for enhanced mechanical properties, J. Polym. Eng. 36 (2016) 53–64.
[19] D. Zhang, L. Shi, J. Fang, X. Li, K. Dai, Preparation and modification of carbon nanotubes, Mater. Lett. 59 (2005) 4044–4047.
[20] S.-Y. Chen, J.-T. Lue, Temperature dependence of interface barrier height change as implicated by field emission studies of aligned-multiwall carbon nanotubes, Phys. Lett. 309 (2003) 114–120.
[21] A.G. Osorio, I.C.L. Silveira, V.L. Bueno, C.P. Bergmann, H_2SO_4/HNO_3/HCl-Functionalization and its effect on dispersion of carbon nanotubes in aqueous media, Appl. Surf. Sci. 255 (2008) 2485–2489.
[22] S.M. Sze, Physics of Semiconductor Devices, third ed., 2007. New Jersey.
[23] M. Gülnahar, Temperature dependence of current-and capacitance-voltage characteristics of an Au/4H-SiC Schottky diode, Superlattice. Microst. 76 (2014) 394–412.
[24] H. Altan, M. Özer, H. Ezgin, Investigation of electrical parameters of Au/P3HT: PCBM/n-6H–SiC/Ag Schottky barrier diode with different current conduction models, Superlattice. Microst. 146 (2020) 106658.
[25] T. Güzel, A.K. Bilgili, M. Özer, Investigation of inhomogeneous barrier height for Au/n-type 6H-SiC Schottky diodes in a wide temperature range, Superlattice. Microst. 124 (2018) 30–40.
[26] A. Sefaoğlu, S. Duman, S. Doğan, B. Gürbulak, S. Tüzemen, A. Türüt, The effects of the temperature and annealing on current-voltage characteristics of Ni/n-type 6H-SiC Schottky diode, Microelectron. Eng. 85 (2008) 631–635.
[27] A. Kaya, Ö. Sevgili, S. Altındal, M.K. Öztürk, Current-conduction mechanism in Au/n-4H-SiC Schottky barrier diodes, Indian J. Pure Appl. Phys. 15 (2015) 56–65.
[28] E.H. Rhoderick, R.H. Williams, Metal-Semiconductor Contacts, Clarendon Press, Oxford, 1988.
[29] X. Zhou, B.L. Langsdorf, F.E. Jones, M.C. Lonergan, Electrochemical tuning of indium phosphide|poly(acetylene) interfaces, Inorg. Chim. Acta. 294 (1999) 207.
[30] S.K. Cheung, N.W. Cheung, Extraction of Schottky diode parameters from forward current-voltage characteristics, Appl. Phys. Lett. 49 (1986) 85–87.
[31] H. Norde, A modified forward I-V plot for Schottky diodes with high series resistance, J. Appl. Phys. 50 (1979) 5052–5053.
[32] S. Chand, J. Kumar, Current transport in Pd_2Si/n-Si(100) Schottky barrier diodes at low temperatures, Appl. Phys. A 63 (1996) 171.
[33] R.T. Tung, Electron transport at metal-semiconductor interfaces: general theory, Phys. Rev. B 45 (1992) 13509–13523.
[34] L.V. Devi, I. Jyothi, R.V. Reddy, Analysis of temperature-dependent Schottky barrier parameters of Cu–Au Schottky contacts to n-InP, Can. J. Phys. 90 (2011) 73–81.
[35] Z.J. Horvath, Comment on "Analysis of I-V measurements on $CrSi_2$/Si Schottky structures in a wide temperature range, Solid State Electron. 39 (1996) 176–178.
[36] W. Yue-Hu, Z. Yi-Men, Z. Yu-Ming, S. Qing-Wen, J. Ren-Xu, Al/Ti/4H-SiC Schottky barrier diodes with inhomogeneous barrier heights, Chin. Phys. B 20 (2011), 087305.
[37] A.K. Bilgili, T. Güzel, M. Özer, Current-voltage characteristics of Ag/TiO_2/n-InP/Au Schottky barrier diodes, J. Appl. Phys. 125 (2019), 035704.

[38] A.A. Kumar, L.D. Rao, V.R. Reddy, C.-J. Choi, Analysis of electrical characteristics of Er/p-InP Schottky diode at high temperature range, Curr. Appl. Phys. 13 (2013) 975–980.
[39] J.H. Werner, H.H. Guttler, Barrier inhomogeneities at Schottky contacts, J. Appl. Phys. 69 (1991) 1522.
[40] M.O. Aboelfotoh, C. Frojdh, C.S. Petersson, Barrier inhomogeneities at Schottky contacts, Phys. Rev. B 67 (2003), 075312.
[41] Y. Goldberg, M.E. Levinshtein, S.L. Rumyantsev, in: M.E. Levinshtein, S. L. Rumyantsev, M.S. Shur (Eds.), Properties of Advanced Semiconductor Materials GaN, AlN, SiC, BN, SiC, SiGe, John Wiley & Sons, Inc., New York, 2001, pp. 93–148.
[42] M.O. Aboelfotoh, Temperature dependence of the Schottky-barrier height of tungsten on *n*-type and *p*-type silicon, Solid State Electron. 34 (1990) 53.
[43] A. Cola, L. Vasanelli, P. Muret, A method for the determination of barrier heights from the capacitance-voltage characteristics of a Schottky junction containing bulk deep traps, Solid State Electron. 38 (1995) 989–995.
[44] A. Singh, K.C. Reinhardt, W.A. Anderson, Temperature dependence of the electrical characteristics of Yb/*p*-InP tunnel metal-insulator-semiconductor junctions, J. Appl. Phys. 68 (1990) 3475.
[45] B. Akkal, Z. Benemara, A. Boudissa, N.B. Bouiadjra, M. Amrani, L. Bideux, B. Gruzza, Modelization and characterization of Au/InSb/InP Schottky systems as a function of temperature, Mater. Sci. Eng. B 55 (1998) 162.
[46] J. R Waldrop, R.W. Grant, Schottky barrier height and interface chemistry of annealed metal contacts to alpha 6H-SiC: crystal face dependence, Appl. Phys. Lett. 62 (1993) 2685–2687.
[47] A. Itoh, H. Matsunami, Analysis of Schottky barrier heights of metal/SiC contacts and its possible application to high-voltage rectifying devices, Phys. Status Solidi 162 (1997) 389–408.